Impact of sulfur dioxide oxidation by Stabilized Criegee Intermediate on sulfate

Golam Sarwar[1]*, Heather Simon[2], Kathleen Fahey[1], Rohit Mathur[1],Wendy S. Goliff[3],William R. Stockwell[4]

[1]Atmospheric Modeling and Analysis Division, National Exposure Research Laboratory, U.S. Environmental Protection Agency, RTP, NC 27711, USA.

[2]Office of Air Quality Planning and Standards, U.S. Environmental Protection Agency, Research Triangle Park, North Carolina, USA.

[3]College of Engineering Center for Environmental Research and Technology, University of California at Riverside, Riverside, CA 92507, USA.

[4]Department of Chemistry, Howard University, Washington, DC 20059, USA.

Corresponding author: Golam Sarwar, U.S. EPA, 109 T.W. Alexander Drive, Research Triangle Park, NC 27711, USA; Tel.: 919-541-2669; fax: 919-541-1379; e-*mail*: sarwar.golam@epa.gov

Abstract

We revise the Carbon Bond chemical mechanism to explicitly represent three Stabilized Criegee Intermediates (SCIs) and their subsequent reactions with sulfur dioxide, water monomer, and water dimer, and incorporate the reactions into the Community Multiscale Air Quality model. The reaction of sulfur dioxide with SCI produces sulfuric acid which partitions into sulfate. We examine the impact of sulfur dioxide oxidation by SCI on sulfate using two different measured rate constants for the reaction of sulfur dioxide and SCI. When we use the higher rate constant and emissions estimates from the Biogenic Emissions Inventory System, it enhances monthly mean sulfate in summer by ~20% in biogenically active areas. Enhancements are driven primarily by SCI produced from the reactions of biogenically derived alkenes and ozone. The use of the lower rate constant only marginally enhances sulfate since it is 65 times lower than the higher rate constant. We performed several sensitivity analyses to investigate the impacts of uncertain biogenic emissions and SCI loss rates. When we use the higher rate constant and emissions estimates from the Model of Emissions of Gases and Aerosols from Nature, it enhances monthly mean sulfate by ~75%. A simulation using the lowest reported rate constant for the reaction of SCI and water indicated the maximum enhancement of sulfate from this chemistry was up to 4 $\mu g/m^3$ over a 24-hour period in some locations in the Southeastern U.S.. Predictions without the SCI reaction are lower than observed sulfate while predictions with the SCI reaction improve the agreements with observations.

Keywords: Stabilized Criegee Intermediate; alkene; ozone; sulfur dioxide; sulfate; water; oxidation

1. INTRODUCTION

Aerosols cause adverse health impacts (Pope et al., 2002), degrade atmospheric visibility (Malm et al., 1994), and alter Earth's energy balance (Murphy et al., 2009). Sulfate (SO_4^{2-}) is an important component of atmospheric aerosols, comprising up to 60% of atmospheric aerosols in the U.S (Hand et al., 2012). SO_4^{2-}primarily forms from gas- and aqueous-phase oxidation of sulfur dioxide (SO_2) by various atmospheric oxidants (Seinfeld and Pandis, 2006). Gas-phase oxidation by hydroxyl radical (HO) and aqueous-phase oxidation by hydrogen peroxide are thought to produce the majority of atmospheric SO_4^{2-} (Sofen et al., 2011).

Calvert and Stockwell (1983) first proposed that the reactions of Stabilized Criegee Intermediate (SCI) with SO_2 are important for production of organic acids and sulfate and incorporated the reactions into the Regional Acid Deposition Mechanism (Stockwell, 1986). These studies found that SCI intermediates could be important oxidants for SO_2 at high VOC to NO_x ratios (VOC= Volatile Organic Compounds and NO_x = Oxides of Nitrogen) and at low relative humidity. Recent laboratory and field experiments (Welz et al., 2012; Mauldin et al., 2012; Carlsson et al., 2012; Taatjes et al., 2013) more strongly show that Criegee Intermediates can oxidize SO_2 to SO_4^{2-}. Welz et al. (2012) studied the reaction of SO_2 and formaldehyde oxide (CH_2OO) using direct measurement technique and measured a rate constant of 3.9×10^{-11} cm^3 $molecule^{-1}$ s^{-1} for the reaction. This value is greater than any other previously reported rate constant. They suggested that SO_2 oxidation by Criegee Intermediates can enhance SO_4^{2-} by as much as SO_2 oxidation by the HO pathway. Mauldin et al. (2012) reported a lower rate constant of 6.0×10^{-13} cm^3 $molecule^{-1}$ s^{-1} for the oxidation of SO_2 by Criegee Intermediate though they used different Criegee Intermediates than the study of Welz et al. (2012). They suggested that oxidation of SO_2 by HO alone could not explain the observed SO_4^{2-} in a boreal forest in Finland. However, the oxidation of SO_2 by HO and SCI was sufficient to explain the SO_4^{2-} observed in their measurements in boreal forests. Carlsson et al. (2012) performed experiments in a static variable pressure reaction chamber to study particle formation during ozonolysis of β-pinene and 2-butene. They measured rate constant similar to the value reported by Welz et al. (2012) and suggested that it provides a reliable estimate for substituted and larger SCI. Taatjes et al. (2013) directly measured rate constants for the oxidation of SO_2 by two conformers of acetaldehyde oxide (*syn*-CH_3CHOO and *ant*-CH_3CHOO). They also reported high rate constant (similar to the

findings of Welz et al., 2012) and suggested that *ant*-CH_3CHOO is more reactive than *syn*-CH_3CHOO.

The impact of SO_2 oxidation by SCI depends on the relative abundance of SCI (Vereecken et al., 2012). The main loss mechanism of SCI from the atmosphere is its reaction with H_2O. While several recent studies directly measured the rate constant for the SCI + SO_2 reaction, only Welz et al. (2012) and Taatjes et al. (2013) reported the direct measurement of the rate constant for the SCI + H_2O reaction. However, they reported an upper limit, not the actual rate constant. Previous studies determined the rate constant of the SCI + H_2O reaction either by indirect measurements or estimations. Indirect measurements quantified the relative rate to that of the SCI + SO_2 reaction and used it to derive the rate constant for the SCI + H_2O reaction. Since the rate constant of the SCI + SO_2 reaction varied among different studies, the reported rate constant for the SCI + H_2O reaction also varied (Hatakeyama and Akimoto, 1994).

Anglada et al. (2011) and Vereecken et al. (2012) noted that the type of conformer as well as the type of substitution in the SCI affects the rate constant for the reaction of SCI and H_2O. Anglada et al. (2011) used computational chemistry to study reactions of fifteen different SCIs with H_2O and found that rate constants vary by ten orders of magnitude for reactions of substituent carbonyl oxides and H_2O. They reported higher rate constants for the reactions for *anti*-conformers with H_2O than the reactions of *syn*-conformers with H_2O. When both H molecules in formaldehyde oxide were substituted by CH_3, the rate constant was calculated to be ~4×10^{-17} cm^3 $molecule^{-1}$ s^{-1}; however, substituting one H molecule by CH_3 and one H molecule by $CH{=}CH_2$ resulted in significant smaller rate constants between ~3×10^{-19} - 8×10^{-18} cm^3 $molecule^{-1}$ s^{-1}.

Several studies suggest that the SCI loss cannot be fully accounted for with the SCI + H_2O reaction alone and that reactions with water dimers are key to properly characterizing this loss. Ryzkhov and Aryia (2004) suggested that reaction rates of SCI and water dimer [$(H_2O)_2$] are greater than those of SCI and H_2O. Ryzhkov and Ariya (2006) reported that SCI + $(H_2O)_3$ and SCI + $(H_2O)_4$ reactions proceed at much slower rates than SCI + $(H_2O)_2$ reaction [$(H_2O)_3$ = water trimer) and $(H_2O)_4$ = water tetramer]. Based on computational chemistry, Vereecken et al. (2012)

calculated rate constants of the reactions of CH_2OO and $CH_3C(H)OO$ with $(H_2O)_2$ to be five orders of magnitude greater than the corresponding reactions with H_2O. Finally, Long et al. (2011) conducted a theoretical study and reported that experimental rate constant for SCI + H_2O is inconsistent with the theoretical estimates since SCI also reacts with $(H_2O)_2$.

Several studies have incorporated this chemistry into various types of models in order to quantify its effects on atmospheric SO_4^{2-} concentrations. Boy et al. (2013) incorporated SCI into a zero-dimensional model and compared predictions to the measurements in VOC-rich environments from Finland and Germany. They employed reactions of SCI with other compounds [including H_2O but not $(H_2O)_2$] contained in the Master Chemical Mechanism (MCM). They used the Mauldin et al. (2012) reported rate constant for the SCI + SO_2 reaction and suggested that the SO_2 oxidation by SCI contributes up to 50% of the measured atmospheric sulfuric acid (H_2SO_4). Pierce et al. (2012) incorporated the Criegee chemistry into GEOS-Chem, used the Welz et al. (2012) reported rate constant for the SCI + SO_2 reaction, and a rate constant of 1.6×10^{-17} cm^3 $molecule^{-1}$ s^{-1} for the SCI + H_2O reaction following the MCM. They reported that it enhanced predicted global H_2SO_4 production by 4% with as much as 100% increase in H_2SO_4 concentrations in forested regions. Sarwar et al. (2013) used the Community Multiscale Air Quality (CMAQ) model to examine the impact of SO_2 oxidation by SCI on regional SO_4^{2-} concentrations. They used the absolute rate constant for the SCI + SO_2 reaction reported by Welz et al. (2012). In the absence of any direct measurement for the SCI + H_2O reaction, they followed the suggestion of Hatakeyama and Akimoto (1994) and derived a rate constant of 2.0×10^{-15} cm^3 $molecule^{-1}$ s^{-1} for the reaction using the relative rate constant ratio. Using this value for the SCI + H_2O reaction and the Welz et al. (2012) reported value for the SCI + SO_2 reaction, they found that the SCI chemistry does not enhance SO_4^{2-} since most SCI is lost by the reaction with H_2O. However, based on a sensitivity simulation using a lower rate constant for the SCI + H_2O reaction, the study concluded that the SCI + SO_2 pathway would enhance SO_4^{2-} under those conditions. Due to the uncertainty in the SCI + H_2O rate constant, they suggested further investigation. Li et al. (2013) also applied the CMAQ model to examine the role of SCI on sulfate formation over the eastern U.S.. They implemented the MCM into the CMAQ model, utilized 36-km horizontal grid-resolution, and simulated air quality for 10 summer days in 2006. When they used the higher rate coefficient for the reaction of SO_2 + SCI as reported by Welz et

al. (2012) and the lower rate constant for the reaction of H_2O + SCI used in the MCM, mean sulfate concentration increased by up to 18% compared to those obtained with the lower rate constant for the SO_2 + SCI reaction used in the MCM. However, when they used a higher rate constant for the reaction of H_2O + SCI (the same value used by Sarwar et al., 2013), mean sulfate concentration increased by less than 0.5% compared to those obtained with the lower rate constant used in the MCM. The range of reported rate constants for both the SCI + SO_2 and the SCI + H_2O reactions and the resulting range in modeling findings suggest that more work is needed to accurately quantify the impact of this chemistry on the conversion of SO_2 to SO_4^{2-}. Here, we take into account the best current information on both the SCI + SO_2 and SCI + H_2O reaction rates to re-examine the impact of SO_2 oxidation by SCI on SO_4^{2-} using the CMAQ model.

2. METHODOLOGY

2.1 Model framework

The impact of Criegee chemistry on SO_4^{2-} concentrations is characterized by performing two sets of model simulations, one of which includes Criegee oxidation chemistry and the other does not. Differences in the results between the two simulations are attributed to the SO_2 oxidation by SCI. Sarwar et al. (2013) described the details of the CMAQ v5.0.1 model (www.cmascenter. org) (Binkowski and Roselle, 2003; Byun and Schere, 2006) which is also used in this study. The model uses the 2005 Carbon Bond chemical mechanism with updated toluene chemistry (CB05TU) (Whitten et al., 2010).

Model inputs are summarized briefly here. The Weather Research and Forecasting (version 3.3) model (Skamarock et al., 2008) is used to derive meteorological fields. The Sparse Matrix Operator Kernel Emissions (SMOKE) model (Houyoux et al., 2000) is used to prepare model-ready emissions using the 2005 National Emissions Inventory (www.epa.gov/ttn/chief/ net/ 2005_nei_point.pdf). The Biogenic Emissions Inventory System (BEIS) (version 3.14) is used for preparing biogenic emissions (Schwede et al., 2005).

Model simulations are performed for January, July, and August, 2006. January is used as a representative winter month while July and August are used as representative summer months. The model performance statistics for O_3 and $PM_{2.5}$ are similar to those reported by previous investigators (Eder and Yu, 2006; Appel et al., 2007; Foley et al., 2010); thus the model is suitable for examining the impact of the SO_2 oxidation by SCI on SO_4^{2-}.

2.2 Criegee chemistry

In previous analysis, Sarwar et al. (2013) used a single SCI to describe the impact of Criegee chemistry on SO_4^{2}. As indicated earlier, the relative importance of this chemistry depends on the abundance of different SCI species since they have vastly different removal rates from the atmosphere. Here we extend the Criegee chemistry based on MCMv3.2 (Jenkin et al., 1997; Saunders et al., 2003; www.mcm.leeds.ac.uk/MCM) to use three different SCIs due to their different reaction rate constants with H_2O (Anglada et al., 2011). CB05TU contains 6 alkenes (ETH, OLE, IOLE, ISOP, ISPD, TERP) and their reactions with O_3; SCI yields for these reactions are added to CB05TU. In addition, reactions for each of these SCIs with SO_2 and H_2O are added to the chemistry. These reactions are summarized in Table 1.

We use CH_2OO (SCI1) to represent SCI formed from both the reaction ethene (ETH) + O_3 and the reaction of terminal olefins (OLE) + O_3. The SCI yield for the ETH/O_3 reaction described by Sarwar et al. (2013) is consistent with the value used in MCMv3.2 and is also used in this study. The yield of SCI1 formed from the reaction of OLE and O_3 is also taken from Sarwar et al. (2013).

SCI2 is produced from the reaction of O_3 + internal olefin (IOLE), a four carbon lumped alkene chemical species. The reaction of IOLE and O_3 produces an ozonide that breaks down to generate a two carbon SCI (CH_3CHOO). Anglada et al. (2011) suggested two different isomers for CH_3CHOO: s*yn*-CH_3CHOO and *ant*-CH_3CHOO. They reported a rate constant of 3.23×10^{-13} cm^3 $molecule^{-1}$ s^{-1} for the reaction of *ant*-CH_3CHOO with H_2O and a rate constant of 3.23×10^{-18} cm^3 $molecule^{-1}$ s^{-1} for the reaction of s*yn*-CH_3CHOO with H_2O. Here, we use s*yn*-CH_3CHOO (SCI2) to represent the SCI from IOLE/O_3 reaction to minimize the loss of SCI by H_2O and

maximize SO_4^{2-} production, and the yield described by Sarwar et al. (2013). As discussed later, the choice of the rate constant is irrelevant since its impact on SO_4^{2-} production is small.

Following the detailed chemistry in MCMv3.2, we supplement the CB05TU to include SCI yield of isoprene (ISOP). The reaction of ISOP and O_3 produces several different SCIs including CH_2OO (SCI1) and four-carbon SCIs. Several different isomers are possible for the four-carbon SCIs and rate constants of their reactions with H_2O also vary. Anglada et al. (2011) described the rate constants for nine different monomers. Seven of the rate constants are on the order of ~10^{-18} cm^3 $molecule^{-1}$ s^{-1}, one rate constant is ~10^{-13} cm^3 $molecule^{-1}$ s^{-1} while the other rate constant is ~10^{-19} cm^3 $molecule^{-1}$ s^{-1}. We represent the four-carbon SCI by using s*yn*-CH_3-anti-(cis-$CH{=}CH_2$) CHOO (SCI3) following Anglada et al. (2011).

CB05TU uses a lumped species (ISPD) to represent isoprene reaction products. We use SCI3 to represent SCI from the ISPD/O_3 reaction. We apply the procedure described by Carter (1996) for deriving the SCI yield from the ISPD/O_3 reaction. Carter (1996) used 10% of methacrolein (MACR), 60% of methyl vinyl ketone (MVK) and 30% of unsaturated C5-aldeydes to derive parameters for ISPD/O_3 reaction. We use the SCI yields in MCMv3.2 for reactions of MACR and MVK with O_3. For the SCI yield of unsaturated C5-aldeyde/O_3 reaction, we use the value of MACR/O_3 reaction. Such assumptions have been used in developing other chemical mechanisms (Goliff et al., 2013).

We follow the detailed chemistry in MCMv3.2 to refine the SCI of TERP/O_3 reaction and their yields. Carter (2000) described the chemistry of TERP using weighted averaging of α-pinene, β-pinene, d-limonene, 3-carene, and sabinene. We use the SCI yields in MCMv3.2 for reactions of O_3 with α-pinene, β-pinene, and d-limonene. The detailed chemistry of 3-carene is not available in MCMv3.2. Ma et al. (2008) conducted chamber experiments involving 3-carene and O_3 and suggested that SCI yield of 3-carene should be lower than that of α-pinene. We use the SCI yield of α-pinene for 3-carene. The detailed chemistry of sabinene is not available. However, the structure of sabinene is similar to β-pinene so we use the SCI yield to be the same as that for β-pinene. SCI3 is used to represent SCI from the TERP/O_3 reaction.

For reactions of SO_2 with SCI1, SCI2, and SCI3, we employ a single rate constant reported by Welz et al. (2012). For SCI1 + H_2O we apply the rate constant of 2.40 x 10^{-15} cm^3 $molecule^{-1}$ s^{-1} (Table 1) suggested by Sarwar et al. (2013) which is two times lower than the upper limit measured by Welz et al. (2012) and slightly lower than the theoretical estimates of 3-5 x 10^{-15} cm^3 $molecule^{-1}$ s^{-1} reported by Anglada et al. (2011). However, this value is greater than the value of 1.0 x 10^{-17} cm^3 $molecule^{-1}$ s^{-1} used in MCMv3.2. For SCI2 + H_2O and SCI3 + H_2O we use rate constants of 3.23 x 10^{-18} and 1.97 x 10^{-18} respectively (Angalda et al., 2012). Our rate constant for SCI3 + H_2O is similar to the values of 2.0-6.0 x 10^{-18} cm^3 $molecule^{-1}$ s^{-1} used in MCMv3.2.

We also implement the reactions of SCI1, SCI2, SCI3 with $(H_2O)_2$. Vereecken et al. (2012) reported a rate constant ratio of 3.5 x 10^5 for the reactions of SCI1 with $(H_2O)_2$ and H_2O, 1.6 x 10^5 for the reactions of SCI2 with $(H_2O)_2$ and H_2O, and 4.1 x 10^2 for the reactions of SCI3 with $(H_2O)_2$ and H_2O. We use these ratios to calculate rate constants for the reactions of SCI1, SCI2, and SCI3 with $(H_2O)_2$. Similar to Vereecken et al. (2012), we also constrain the estimated rate constant with a physical upper limit of 1.0 x 10^{-10} cm^3 $molecule^{-1}$ s^{-1}. We calculate $(H_2O)_2$ using $[(H_2O)_2] = K_{eq} \times [H_2O]$ (Shillings et al., 2011), where K_{eq} (0.04 atm^{-1}) is the equilibrium constant for dimer formation (Vereecken et al., 2012). The model uses WRF predicted H_2O mixing ratios. It should be noted that such reactions are not used in MCMv3.2. Previous modeling studies (Boy et al., 2013; Pierce et al., 2012; Sarwar et al., 2013; Li et al., 2013) did not use such reactions either.

While not important, we also implement the reaction of SCI1, SCI2, and SCI3 with NO_2 for completeness (rate constant taken from Welz et al., 2012). SCI can also react with other chemical species; however, they generally do not play substantial roles in affecting the fate of SCI in the atmosphere (Vereecken et al., 2012) and therefore are not considered in this study.

3. RESULTS AND DISCUSSIONS

3.1 Impact of the SO_2 oxidation by SCI on SO_4^{2-}

3.1.1 Domain-wide mean SO_4^{2-} concentrations without and with SCI initiated reaction

The surface-level domain-wide monthly mean SO_4^{2-} concentration obtained without the SCI reactions is 1.11 $\mu g/m^3$ in January, 1.60 $\mu g/m^3$ in July, and 1.59 $\mu g/m^3$ in August. The oxidation of SO_2 by SCI enhances the domain-wide monthly mean SO_4^{2-} concentration by 0.05 $\mu g/m^3$ in January, 0.10 $\mu g/m^3$ in July, and 0.08 $\mu g/m^3$ in August. While the SO_2 oxidation by SCI enhances SO_4^{2-} both in winter and summer months, it produces more SO_4^{2-} in summer than in winter.

3.1.2 Spatial and seasonal variation of the SO_4^{2-} enhancements due to SO_2 oxidation by SCI

Predicted monthly mean SO_4^{2-} concentrations without the SCI initiated reactions and enhancements with the SCI initiated pathway are shown in Figure 1. In winter, the SO_2 oxidation by SCI increases monthly mean SO_4^{2-} in the southeastern U.S. and Mexico by 0.15-0.30 $\mu g/m^3$. However, it increases SO_4^{2-} by 0.15-1.20 $\mu g/m^3$ over a large area across the eastern U.S. during summer months. The impacts are especially pronounced in the southeastern U.S. where summertime enhancements exceed 1.0 $\mu g/m^3$. Criegee chemistry leads to smaller increases in SO_4^{2-} (0.15-0.3 $\mu g/m^3$) in California and other areas in western U.S. during summer months. In addition to causing larger enhancements in SO_4^{2-} in the summer than in the winter, Criegee chemistry also leads to increases over a more extensive geographic area during the summer than during the winter.

In the model simulations, SO_4^{2-} enhancements are primarily the result of the SO_2 oxidation by SCI3 which is produced from the reactions of biogenic derived alkenes and O_3. At 1.0 atm and 50% relative humidity, we calculate that most of SCI1 (>99%) and SCI2 (>90%) are lost by their reactions with H_2O and $(H_2O)_2$ and thus are unavailable for reacting with SO_2. In contrast, only ~10-20% of SCI3 is lost by its reactions with H_2O and $(H_2O)_2$ under similar conditions.

Although not shown here, predicted SCI3 concentrations in winter are small due to low emissions of biogenic precursor VOCs. In contrast during summer, larger biogenic emissions result in much higher simulated SCI3 concentrations. While predicted summertime SCI3 concentrations are lower than HO levels, the production rates of SO_4^{2-} via the SCI initiated reaction are similar to or greater than those with the HO initiated pathway. As a reference, the

rate constant for the reaction of SO_2 + HO at 1.0 atmosphere and 298 K is 9.5 x 10^{-13} cm^3 $molecule^{-1}$ s^{-1}.

3.1.3 Temporal variation of the SO_4^{2-} enhancements

We examine the day-to-day variability of the SCI initiated SO_4^{2-} enhancements by calculating an area-wide daily mean value over 490,000 km^2 in southeastern U.S. [see black rectangle in Figure 1(d)]. Predicted area-wide day-to-day variations in daily mean SO_4^{2-} enhancements due to the SCI reaction are shown in Figure 2a for July. Over this area of the Southeast, the SCI chemistry enhances daily mean summer SO_4^{2-} by 0.2-1.4 $\mu g/m^3$. Day to day variation in SO_4^{2-} enhancements track the product of SO_2 and SCI3 (r = 0.89) (Figure 2a) which supports the conclusion that the SCI3 initiated reaction is responsible for the SO_4^{2-}enhancements. The day-to-day variations in the product of SO_2 and SCI3 are largely driven by variability in SO_2 but are also affected to a lesser extent by day-to-day changes in SCI3.

Monthly average diurnal variations are shown for the same region examined for daily variations (Figure 2b). Predicted SO_4^{2-} concentrations without the SCI initiated pathway are relatively constant throughout the day. Although SO_4^{2-} concentrations are enhanced by Criegee chemistry at all hours, the enhancements are greater at night. This diurnal pattern is driven by the relative availability of the two oxidants. Predicted HO concentrations are relatively small at night and peak during the day while predicted SCI3 concentrations are relatively constant. Predicted SCI3 concentrations are greater than the nighttime HO values leading to greater nighttime production rates of SO_4^{2-} via the SCI initiated pathway than via the HO initiated pathway. Conversely, predicted SCI3 concentrations are substantially lower than the daytime HO values, causing daytime production rates of SO_4^{2-} to come predominantly from the HO initiated pathway.

3.2 Impact of the SCI initiated SO_2 oxidation on SO_4^{2-} with alternate biogenic emissions estimates

Since the SCI initiated SO_2 oxidation enhances more SO_4^{2-} in summer, we performed two additional simulations in July using biogenic emissions inputs derived from the Model of Emissions of Gases and Aerosols from Nature (Guenther et al., 2012): one without the SCI initiated reaction and one with the SCI initiated reactions. Predicted monthly mean SO_4^{2-}

concentrations from the MEGAN sensitivity without the SCI initiated reaction and related enhancements are presented in Figure 3. The domain-wide monthly mean SO_4^{2-} concentration obtained without the SCI initiated reaction is 1.53 $\mu g/m^3$ (slightly lower than the 1.6 $\mu g/m^3$ obtained using BEIS emissions). The SCI initiated reaction enhances the domain-wide monthly mean SO_4^{2-} by 0.20 $\mu g/m^3$ (twice as much as the enhancement with BEIS emissions). With biogenic emissions estimates of MEGAN, the SCI initiated reaction increases SO_4^{2-} concentrations by 1.2-2.4 $\mu g/m^3$ in the eastern U.S., also about two times greater than the enhancements in the eastern U.S. with emissions estimates from BEIS. These differences are due to the much larger eastern U.S. biogenic emissions estimates from MEGAN than from BEIS. Pouliot and Pierce (2008) examined emissions from BEIS and MEGAN and reported that MEGAN produces 60% more isoprene emissions than those from BEIS. Carlton and Baker (2011) compared modeled isoprene concentrations to measurements in the Ozark mountains and reported that MEGAN emissions led to model over-predictions of surface isoprene while BEIS emissions led to model under-predictions of surface isoprene. Hogrefe et al. (2011) also studied the impact of biogenic emission uncertainties on ozone and fine particulate matter in eastern U.S. and reported that MEGAN estimated biogenic emissions are much greater than those estimated by BEIS. Predicted isoprene concentrations with MEGAN estimated emissions were much greater than the observed levels while predicted isoprene concentrations with BEIS estimated emissions were closer to the observed levels. The increased biogenic VOC concentrations affect SO_4^{2-} chemistry in several ways. First, HO levels are somewhat depressed in the MEGAN case due to more loss via HO + VOC reactions. Predicted H_2O_2 levels are greater with the MEGAN case. These lead to slightly lower SO_4^{2-} concentrations when no Criegee chemistry was simulated. Second, and more significantly, increased biogenic emissions lead to enhanced SCI3 levels. Collectively, these suggest that the simulated relative importance of Criegee chemistry on SO_4^{2-} formation is heavily dependent on biogenic emissions estimates.

3.3 Impact of the SO_2 oxidation by SCI with alternative rate constants

We performed a series of four sensitivity simulations to investigate the impact of uncertain rate constants involving SCIs. First, an additional simulation using BEIS estimated emissions was completed with the lower rate constant reported by Mauldin et al. (2012) for the SCI3 + SO_2 reaction (65 times slower than the Welz et al., 2012 value). The rate constants for SCI1 + SO_2

and SCI2 + SO_2 reactions are not changed for this simulation. Mauldin et al. (2012) did not report any rate constant for the reaction of SCI and H_2O; thus, we assume the rate constants in Table 1 for this sensitivity. The use of the lower rate constant for the SCI3 + SO_2 reaction only marginally increases SO_4^{2-} concentrations. For example, daily mean SO_4^{2-} concentrations without the SCI initiated reaction and enhancements obtained with the SCI initiated reaction for July 1 are shown in Figure 4(a-b). Daily mean enhancements obtained with the lower rate constant ranged from 0.05-0.15 $\mu g/m^3$, compared to enhancements of up to 0.3-2.6 $\mu g/m^3$ in the original simulation (Figure 4(c)).

Boy et al. (2013) implied that Mauldin et al. (2012) value is not an absolute rate constant for the reaction of SCI with SO_2, but rather an effective rate constant for SO_4^{2-} production by the SCI reaction that already accounts for the loss with other chemical compounds. Thus, we perform a second sensitivity simulation using SCI3 + SO_2 and without any reactions of SCI3 with H_2O, $(H_2O)_2$, and NO_2. The resulting daily mean SO_4^{2-}enhancements for July 1 are shown in Figure 4(d). This new "net" reaction rate produces SO_4^{2-} enhancements that are ~2 times greater than the enhancements obtained with the higher rate constant of Welz et al. (2012). Thus, further clarification on the use of the lower rate constant reported by Mauldin et al. (2012) is needed.

Third, as indicated earlier, Anglada et al. (2011) calculated rate constants for the reactions of different SCIs and H_2O. The lowest calculated value was 2.93×10^{-19} molecules cm^{-3} s^{-1}. We performed another simulation by using this lowest value for the rate constant for the reaction of SCI3 and H_2O and by additionally adjusting the rate constant for the reaction of SCI3 and $(H_2O)_2$. All other conditions were unchanged. Predicted daily mean sulfate enhanced by ~1.8-4.0 $\mu g/m^3$ in the southeast U.S. (Figure 4(e)) while the enhancements obtained with the higher rate constant for SCI3 and H_2O were ~1.0-2.6 $\mu g/m^3$ in the southeast U.S. (Figure 4(c)). Thus, the use of the lower rate constant for SCI3+H_2O produces substantially greater sulfate which further emphasizes the role that the SCI3/water reaction plays in enhancing sulfate.

Vereecken et al. (2012) suggested that SCIs can also undergo unimolecular decomposition and reported first order rate constants for their reactions. The fourth sensitivity simulation was performed by accounting for unimolecular decomposition of SCI1, SCI2, and SCI3 with the

following first order rate constants: 0.30 s^{-1} for SCI1 (Fenske et al., 2000), 0.388 s^{-1} for SCI2 (Vereecken et al., 2012), and 0.21 s^{-1} for SCI3 (Vereecken et al., 2012). For this simulation, we used the lowest rate constant for the reaction of SCI3 and H_2O and appropriately adjusted the rate constant for the reaction of SCI3 and $(H_2O)_2$ as was done for sensitivity #3 described in this section. Predicted daily mean sulfate enhancements are shown in Figure 4(f) and ranged between ~1.2-3.5 $\mu g/m^3$ in the southeast U.S.. Enhancements decreased by up to ~0.5 $\mu g/m^3$ compared to the enhancements obtained with the lower rate constant for the reaction of SCI3 and H_2O alone as shown in Figure 4(e) due to the loss of SCI3 via unimolecular decomposition. This further underscores the need for accounting all important loss pathways of SCI for accurately examining the impact of SCI initiated SO_2 oxidation on sulfate.

3.4 Comparison of predicted SO_4^{2-} with observed data

Comparisons with ambient data are conducted to determine whether Criegee chemistry produces more realistic modeled SO_4^{2-} concentrations. Comparisons are made between modeled and observed values at monitoring locations in the Eastern U.S. defined by the black rectangles in Figure 1(d) and Figure 3(b) for the BEIS and MEGAN cases, respectively. Measurements came from the Clean Air Status and Trends Network (CASTNET), the Interagency Monitoring of Protected Visual Environments (IMPROVE), the Chemical Speciation Network (CSN), and the Southeastern Aerosol Research and Characterization (SEARCH) monitoring sites in southeastern U.S.. It should be noted that CASTNET measurements are reported as weekly averages while IMPROVE and CSN measurements are reported as daily averages once every three days. SEARCH measurements are made hourly but were aggregated to 24-hour averages for this analysis for comparison with other networks. Figure 5 shows that model predictions without the SCI initiated pathway are lower than the observed data for CASTNET, IMPROVE, and CSN monitoring networks (BEIS emissions) while predictions obtained with the SCI initiated pathway generally agree better with the observed concentrations. At the SEARCH sites, the results are mixed than for the measurements made in other networks. Although the SO_4^{2-} predicted in the base simulation (BEIS emissions) was generally lower than observed concentrations, there are a few time periods in which the model over-predicted SO_4^{2-}. During times of model under-predictions, the SCI initiated pathway tends to improve model predictions but during the less frequent period of model over-predictions, the Criegee chemistry degrade performance slightly.

Similar improvements in model performance are seen in the MEGAN case for CASTNET, IMPROVE, and CSN monitoring sites. At SEARCH sites, the Criegee chemistry sometime improved performance but also sometimes lead to model over-predictions for SO_4^{2-} similar in magnitude to the under-predictions in the base simulation. In the BEIS simulations, the model underestimation of SO_4^{2-} concentrations persists despite the Criegee enhancements. In contrast, this model underestimation in the MEGAN simulations is largely eliminated by the Criegee enhancements. As previously indicated, MEGAN estimated biogenic emissions are much higher than those obtained with BEIS and enhanced SO_4^{2-} predictions shown in the Figure 5 are the direct result of these higher biogenic emissions estimates from MEGAN.

Availability of both SO_2 and SO_4^{2-} measurements at the CASTNET and SEARCH sites allows an investigation into the model's ability to capture the amount of conversion from SO_2 to SO_4^{2-}. Figures 6 and 7 compare the observed and predicted mass fraction of sulfur in SO_4^{2-} $\left(\frac{\frac{32\,x\,SO_4}{96}}{\frac{32\,x\,SO_2}{64}+\frac{32\,x\,SO_4}{96}}\right)$ at CASTNET and SEARCH sites, respectively. Mass fractions of sulfur in SO_4^{2-} without the SCI reaction are lower than the observed data which suggests missing SO_2 oxidation pathways in the model. Mass fractions of sulfur in SO_4^{2-} with the SCI initiated SO_2 reaction are slightly greater than those obtained without the SCI reaction in the BEIS case and substantially greater in the MEGAN case. For all simulations, the addition of Criegee chemistry brings the amount of SO_2 conversion closer to observations. However, the modeled mass fraction is still lower than the measured fraction, suggesting either additional missing chemical pathways or underestimates of reaction rates or oxidant concentrations. Note that iron and manganese catalyzed aqueous SO_2 oxidation is already included in the model, but uncertainty in this chemical pathway or underestimated cloud presence could also contribute to the underestimated mass fraction on cloudy days when aqueous-phase chemistry is important for SO_4^{2-} formation. Average cloud coverage was similar in July and August. However, cloud coverage was more prevalent in January than in July or August. In January, more cloudiness existed in north central area of the modeling domain. Predicted SO_2 concentrations are generally higher than the observed values as shown by comparing the predictions of SO_4^{2-} in Figure 5 with the under predictions of the mass fraction of sulfur in Figures 6 and 7.

4. SUMMARY AND CONCLUSION

This work examines the impact of SO_2 oxidation by SCI on SO_4^{2-} using two different rate constants and two different biogenic emissions estimates. When the higher rate constant is used, Criegee chemistry enhances the domain-wide monthly mean SO_4^{2-} by 4.5% in winter and 5-6% in summer. However, enhancements are much larger in regions with significant biogenic VOC emissions. The use of MEGAN estimated biogenic emissions results in larger enhancements of SO_4^{2-} compared to simulations using BEIS estimated emissions which also suggests the need for further evaluation of emissions estimates from the two models. Substantial uncertainty in rate constants for both the SCI + SO_2 and SCI + H_2O and SCI + $(H_2O)_2$ reactions lead to a wide range of possible impacts.

Our results obtained with the higher rate constant reported by Welz et al. (2012) for the SO_2 + SCI reaction and the lower rate constant for the H_2O + SCI3 reaction reported by Anglada et al. (2011) are consistent with the suggestion of Welz et al. (2012) who noted that Criegee reactions can substantially enhance SO_4^{2-}. Our results are also similar to the findings of Pierce et al. (2012) who reported that it enhances SO_4^{2-} appreciably in forested regions but not in un-forested regions. Our results obtained with the BEIS emissions are consistent to the findings of Li et al. (2013) while impacts obtained with the MEGAN emissions are greater than the Li et al. (2013) results. However, these new findings contrast to those reported by Sarwar et al. (2013), who found that Criegee reactions minimally enhance SO_4^{2-}. The driver for these different findings is the use of different rate constant for SCI3 + H_2O reaction.

Our results with the lower rate constant reported by Mauldin et al. (2012) for the SO_2 + SCI reaction and the lower rate constant for the H_2O + SCI3 reaction reported by Anglada et al. (2011) are different than the findings of Mauldin et al. (2012) and Boy et al. (2013) who reported that this reaction substantially enhances SO_4^{2-} in Finland and Germany. Possible reasons for such inconsistent results include differences in the model used in the two studies, differences in the rate constant used for the H_2O + SCI3 reaction, and not accounting for the loss of SCI3 by the reaction with $(H_2O)_2$. When we use the lower rate constant reported by Mauldin et al. (2012) for the SO_2 + SCI reaction without any loss of SCI3 by water, it enhances SO_4^{2-} which warrants clarification on the use of the lower rate constant reported by Mauldin et al. (2012).

Results of this and other recent studies suggest that the SO_2 oxidation by SCI enhances SO_4^{2-} when both SO_2 and biogenically derived SCI are simultaneously present. Such enhancements occur due to the use of the high rate constant for the SO_2 + SCI reaction and the low rate constant for the H_2O + SCI3 reaction. While the high rate constant for the SO_2 + SCI reaction has been measured, the low rate constant for the H_2O + SCI3 reaction is based on theoretical study (Anglada et al., 2011). We believe the results presented, herein, are the upper limit of the impact of the SO_2 oxidation by SCI since a low rate constant for the H_2O + SCI3 reaction was used and hope this study motivates others to measure rate constant for the H_2O + SCI3 reaction.

DISCLAIMER

Although this paper has been reviewed by EPA and approved for publication, it does not necessarily reflect EPA's policies or views.

References

Anglada, J. M., Gonzalez, J., Torrent-Succarrat, M., 2011. Effects of substituents on the reactivity of carbonyl oxides. A theoretical study on the reaction of substituted carbonyl oxides with water. Phys. Chem. Chem. Phys., 13, 13034-13045.

Appel, K. W., Gilliland, A. B., Sarwar, G., Gilliam, R. C, 2007. Evaluation of the Community Multiscale Air Quality (CMAQ) model version 4.5: Sensitivities impacting model performance, Part I-Ozone. Atmos. Environ., 41, 9603–9615.

Binkowski, F. S., Roselle, S. J., 2003. Community Multiscale Air Quality (CMAQ) model aerosol component, I: Model description. J. Geophys. Res.,108, 4183, doi:10.1029/2001JD001409.

Boy, M., Mogensen, D., Smolander, S., Zhou, L., Nieminen, T., Paasonen, P., Plass-Dulmer, C., Sipila, M., Petaja, T., Mauldin, L., Berresheim, H., Kulmala, M., 2013. Oxidation of SO_2 by stabilized Criegee Intermediate (sCI) radicals as a crucial source for atmospheric sulfuric acid concentrations. Atmospheric Chemistry & Physics, 13, 3865-3879.

Byun, D., Schere, K. L, 2006. Review of the governing equations, computational algorithms, and other components of the Models-3 Community Multiscale Air Quality (CMAQ) Modeling System. Applied Mechanics Reviews, 59, 51-77.

Calvert, J. G., Wtockwell, W.R., 1983. Acid Generation in the Troposphere by Gas Phase Chemistry. Environmental Science & Technology, 17, 428A - 443A.

Carlsson, P.T.M., Keunecke, C., Kruger, B. C., Maab, M.C., Zeuch, T., 2012. Sulfur dioxide oxidation induced mechanistic branching and particle formation during the ozonolysis of β-pinene and 2-butene. Phys. Chem. Chem. Phys., 14, 15637-15640.

Carlton, A.G., Baker, K., 2011. Photochemical Modeling of the Ozark Isoprene Volcano: MEGAN, BEIS, and Their Impacts on Air Quality Predictions. Environmental Science &Technology, 45, 4438-4445.

Carter, W. P. L., 1996. Condensed atmospheric photooxidation mechanisms for isoprene. Atmospheric Environment, 30, 4275-4290.

Carter, WPL, 2000. Implementation of the SAPRC-99 chemical mechanism into the Models-3 Framework, report to the United States Environmental Protection Agency. Available at www.cert.ucr.edu/~carter/pubs/s99mod3.pdf (last accessed on May 18, 2013).

Eder, B., S. Yu, 2006. A performance evaluation of the 2004 release of Models-3 CMAQ. Atmospheric Environment, 40, 4811-4824.

Fenske, J. D., Hasson, A.S., Ho, A.W., Paulson, S.E., 2000. Measurement of absolute unimolecular and bimolecular rate constants for CH3CHOO generated by the trans-2-butene reaction with ozone in the gas phase. Journal of Physical Chemistry A 104, 9921-9932.

Foley, K. M., Roselle, S.J., Appel, K.W., Bhave, P.V., Pleim, J.E., Otte, T. L., Mathur, R., Sarwar, G., Young, J.O., Gilliam, R.C., Nolte, C.G., Kelly, J.T., Gilliland, A.B., Bash, J.O., 2010. Incremental testing of the Community Multiscale Air Quality (CMAQ) modeling system version 4.7. Geosci. Model Dev., 3, 205–226.

Goliff, W.S., Stockwell, W.R., Lawson, C.V., 2013. The Regional Atmospheric Chemistry Mechanism, Version 2, Atmospheric Environment, 68, 174-185.

Guenther, A. B., Jiang, X., Heald, C. L., Sakulyanontvittaya, T., Duhl, T., Emmons, L. K., Wang, X., 2012. The Model of Emissions of Gases and Aerosols from Nature version 2.1 (MEGAN2.1): an extended and updated framework for modeling biogenic emissions, Geosci. Model Dev. Discuss., 5, 1503-1560, doi:10.5194/gmdd-5-1503-2012.

Hand, J.L., Schichtel, B.A., Pitchford, M., Malm, W.C., Frank, N.H., 2012. Seasonal composition of remote and urban fine particulate matter in the United States. Journal of Geophysical Research, 117, D05209, doi:10.1029/2011JD017122.

Hatakeyama, S., Akimoto, H., 1994. Reactions of Criegee intermediates in the gas-phase. Research Chemical Intermediates, 20, 503-524.

Hogrefe, et al., 2011. Impact of biogenic emission uncertainties on the simulated response of ozone and fine particulate matter to anthropogenic emission reductions. Journal of Air & Waste Management Association, 61:92-108, DOI:10.3155/1047-3289.61.1.92.

Houyoux, M. R., Vukovich, J. M., Coats Jr., C. J., Wheeler, N. M., Kasibhatla, P. S., 2000. Emission inventory development and processing for the seasonal model for regional air quality (SMRAQ) project. J. Geophys. Res., 105, 9079–9090.

Jenkin, M.E., Saunders, S.M., Pilling, M.J., 1997. The tropospheric degradation of volatile organic compounds: A protocol for mechanism development. Atmospheric Environment, 31, 81-104.

Li, J., Ying, Q., Yi, B., Yang, P., 2013. Role of Stabilized Criegee Intermediates in the formation of Atmospheric Sulfate in Eastern United States. Atmospheric Environment, 79, 442-447.

Long, B., Tan, X., Long, Z., Wang, Y., Ren, D., Zhang, W., 2011. Theoretical studies on reactions of the stabilized H_2COO with HO_2 and the $HO_2…H_2O$ complex. J. of Physical Chemistry A, 115, 6559-6567.

Ma., Y., Porter, R.A., Chappell, D., Russell, T., 2009. Mechanisms for the formation of organic acids in the gas-phase ozonolysis of 3-carene. Phys. Chem. Chem. Phys., 11, 4184-4197.

Malm, W., Sisler, J.F., Huffman, D., Eldred, R. A., Cahil, T.A., 1994. Spatial and seasonal trends in particle concentration and optical extinction in the United States. Journal of Geophysical Research, 114, 99, No. D1, 1347-1370.

Mauldin III, R.L., Berndt, T., Sipilä, M., Paasonen, P., Petäjä, T., Kim, S., Kurtén, T., Stratmann, T. F., Kerminen V. M., Kulmala, M., 2012. A new atmospherically relevant oxidant of sulphur dioxide. Nature, 488, 193-197.

Murphy, D. M., Solomon, S., Portmann, R.W., Rosenlof, K.H., Forster, P.M., Wong, T., 2009. An observationally based energy balance for the Earth since 1950. Journal of Geophysical Research, 114, D17107, doi:10.1029/2009JD012105.

Pierce, J. R., Evan, M. J., Scott, C. E., Andrea, D. D., Farmer, D. K., Swietlicki, E., Spracklen., D. V., 2013. Weak sensitivity of cloud condensation nuclei and the aerosol indirect effect to Criegee + SO_2 chemistry. Atmospheric Chemistry & Physics, 13, 3163-3176.

Pope III, C.A., Burnett, R.T., Thun, M.J., Calle, E.E., Krewski, D., Ito, K., Thurston, G.D., 2002. Lung cancer, cardiopulmonary mortality, and long term exposure to fine particulate air pollution. Journal of the American Medical Association, 287, 1132-141.

Pouliot, G., Pierce, T., 2008. A tale of two models: a comparison of the Biogenic Emission Inventory System (BEIS3.14) and Model of Emissions of Gases and Aerosols from Nature (MEGAN 2.04). 7th Annual CMAS Models-3 Users' Conference, October 6-8, 2008, UNC-Chapel Hill, NC.

Ryzhkov, A.B., Ayiya, P.A., 2004. A theoretical study of the reactions of parent and substituted Criegee intermediates with water and water dimer. Physical Chemistry Chemical Physics, 6, 5042-5050.

Ryzhkov, A.B., Ayiya, P.A., 2006. The importance of water clusters $(H_2O)_n$ (n=2,..4) in the reaction of Criegee intermediates with water in the atmosphere. Chemical Physics Letter, 419, 479-485.

Sarwar, G., Fahey, F., Kwok, R., Gilliam, R., Xue, J., Jianzhen, Y., Carter, W. P. L., 2013. Potential Impacts of two SO_2 oxidation pathways on regional sulfate concentrations: aqueous-phase oxidation by NO_2 and gas-phase oxidation by Stabilized Criegee Intermediates. Atmospheric Environment, 68, 186-197.

Saunders, S.M., Jenkin, M.E., Derwent, R.G., Pilling, M.J., 2003. Protocol for the development of the Master Chemical Mechanism, MCM v3 (Part A): tropospheric degradation of non-aromatic volatile organic compounds. Atmospheric Chemistry and Physics, 3, 161-180.

Schwede, D., Pouliot, G., Pierce, T., 2005. Changes to the biogenic emissions inventory system version 3 (BEIS3). 4th Annual CMAS Models-3 Users' Conference, September 26-28, 2005, UNC-Chapel Hill, NC.

Shillings, A. J .L., Ball, S. M., Barber, M. J., Tennyson, J., Jones, R. L., 2011. An upper limit for water dimer absorption in the 750 nm spectral region and a revised water line list. Atmospheric Chemistry & Physics, 11, 4237-4287.

Seinfeld, J. H., Pandis, S. N., 2006. Atmospheric chemistry and Physics, Willey Express, 2006.

Skamarock, W. C., Klemp, J. B., Dudhia, J., Grill, D. O., Barker, D. M., Duda, M. G, Huang, X-Y, Wang, W., Powers, J. G., 2008. A description of the advanced research WRF version 3. NCAR Tech Note NCAR/TN 475 STR, 2008, 125 pp. [Available from UCAR Communications, P.O. Box 3000, Boulder, CO 80307.]

Sofen, E. D., Alexander, B., Kunasek, A., 2011. The impact of anthropogenic emissions on atmospheric sulfate production pathways, oxidants, and ice core Δ^{17} $O(SO^{2-}_4)$. Atmospheric Chemistry & Physics, 11, 3565–3578.

Stockwell, W.R., 1986. A Homogeneous Gas Phase Mechanism for use in a Regional Acid Deposition Model. Atmos. Environ., 20, 1615-1632.

Taatjes, C. A., Welz, O., Eskola, A. J., Savee, J. D., Scheer, A. M., Shallcross, D. E., Rotavera, B., Lee, E. P. F., Dyke, J. M., Mok, D. K. W., Osborn, D. L., Percival, C. J., 2013. Direct Measurements of Conformer Dependent Reactivity of the Criegee Intermediate CH3CHOO. Science, 340, 177-180.

Vereecken, L., Harder, H.; Noveli, A., 2012. The reaction of Criegee intermediates with NO, RO_2, and SO_2, and their fate in the atmosphere, Phys. Chem. Chem. Phys., 14, 14682-14695.

Welz, O., Savee, J.D., Osborn, D.L., Basu, S.S., Percival, C. J., Shallcross, D.E., Taatjes, C.A., 2012. Direct kinetic measurements of Criegee Intermediate (CH_2OO) formed by reaction of CH_2I with O_2. Science, 335, 204-207.

Whitten, G. Z., Heo, G., Kimura, Y., McDonald-Buller, E., Allen, D., Carter, W.P.L, Yarwood, G., 2010. A new condensed toluene mechanism for Carbon Bond: CB05-TU. Atmospheric Environment, 44, 5346-5355.

Table 1: Criegee chemistry for CB05TU mechanism

Reaction No.	Reaction	Rate constant (cm^3 $molecule^{-1}$ s^{-1})	Note
118	O_3 + OLE =… + 0.319*SCI1	Yarwood et al. (2005)	Sarwar et al., 2013
122	O_3 + ETH = … + 0.37*SCI1	Yarwood et al. (2005)	Sarwar et al., 2013
126	O_3 + IOLE = … + 0.316*SCI2	Yarwood et al. (2005)	Sarwar et al., 2013
159	O_3 + ISOP = … + 0.11*SCI1 + 0.11*SCI3	Yarwood et al. (2005)	Used isoprene chemistry in MCMv3.2
162	O_3 + ISPD = … + 0.2022*SCI1 + 0.0806*SCI3	Yarwood et al. (2005)	Used weighted average of MACR/MVK rxns in MCM
167	O_3 + TERP = … + 0.0518*SCI1 + 0.1592*SCI3	Yarwood et al. (2005)	Derived following MCMv3.2
CR01	SCI1 + SO_2 = SULF	3.90×10^{-11}	Welz et al., 2012
CR02	SCI2 + SO_2 = SULF	3.90×10^{-11}	Welz et al., 2012
CR03	SCI3 + SO_2 = SULF	3.90×10^{-11}	Welz et al., 2012
CR04	SCI1 + H_2O =	2.40×10^{-15}	Sarwar et al., 2013
CR05	SCI2 + H_2O =	3.23×10^{-18}	Anglada et al., 2011
CR06	SCI3 + H_2O =	1.97×10^{-18}	Anglada et al., 2011
CR07	SCI1 + $(H_2O)_2$ =	1.00×10^{-10}	Vereecken et al., 2012
CR08	SCI2 + $(H_2O)_2$ =	5.17×10^{-13}	Vereecken et al., 2012
CR09	SCI3 + $(H_2O)_2$ =	8.08×10^{-16}	Vereecken et al., 2012
CR10	SCI1 + NO_2 = NO_3	7.00×10^{-12}	Welz et al., 2012
CR11	SCI2 + NO_2 = NO_3	7.00×10^{-12}	Welz et al., 2012
CR12	SCI3 + NO_2 = NO_3	7.00×10^{-12}	Welz et al., 2012

Note:
O_3 = ozone, OLE = terminal alkenes, ETH=ethene, IOLE = internal alkenes, ISOP = isoprene, ISPD = isoprene reaction product, TERP = monoterpene, SCI1 = H_2COO (Anglada et al., 2011 and Vereecken et al., 2012), SCI2 = s*yn*-CH_3CHOO (Anglada et al., 2011 and Vereecken et al., 2012), SCI3 = s*yn*-CH_3-anti-(cis-$CH{=}CH_2$) CHOO (Anglada et al., 2011 and Vereecken et al., 2012), SO_2 = sulfur dioxide, SULF = sulfuric acid, NO_2 = nitrogen dioxide , NO_3 = nitrate radical, H_2O = water monomer, $(H2O)_2$ = water dimer, MCM = Master Chemical Mechanism.

OLE is a lumped species, represents terminal olefins, and is composed of two carbons. Sarwar et al. (2013) derived a yield of 0.319 for OLE. However, they used only one SCI in the mechanism. Since three SCIs are used here, we use O_3 + OLE =0.319*SCI1.

ETH represents ethene and is composed of two carbons. Sarwar et al. (2013) derived a yield of 0.37 for ETH which is consistent with the value used in MCM. However, they used only one SCI in the mechanism. Since three SCIs are used here, we use O_3 + ETH =0.37*SCI1.

IOLE is a lumped species, represents internal olefins, and is composed of four carbons. Sarwar et al. (2013) derived a yield of 0.316 for IOLE. However, they used only one SCI in the mechanism. Since three SCIs are used here, we use O_3 + IOLE = 0.316*SCI2.

ISOP represents isoprene for which Sarwar et al. (2013) derived a yield of 0.354. Here, we calculate the yields following MCM: O_3 + ISOP = 0.11*SCI1 + 0.11*SCI3.

ISPD is a lumped species, represents isoprene reaction products (methyl acrolein, methyl vinyl ketone, unsaturated aldehydes, etc.) and is composed of four carbons. Based on MCM, we derive following yields for methyl acrolein: O_3 + METHYL ACROLEIN = 0.3256*SCI1 + 0.0216*SCI3 and methyl vinyl ketone: O_3 + MVK = 0.12*SCI1 + 0.12*SCI3. Sarwar et al. (2013) derived a yield of 0.472 for ISPD. Here we use weighted average yields of methyl acrolein, methyl vinyl ketone, and unsaturated aldehydes following Carter (1996): O_3 + ISPD = 0.1045*SCI1 + 0.0741*SCI3. We use 10% for methyl acrolein, 60% for methyl vinyl ketone, 30% for unsaturated aldehydes. SCI yields for unsaturated aldehydes were taken equal to those of methyl acrolein.

TERP is a lumped species, represents monoterpenes, and is composed of ten carbons. Sarwar et al. (2013) derived a yield of 0.268 for TERP. Here, we use the following equation to calculate SCI yield for TERP (Carter, 2000):
SCI yield for TERP = 0.4*APINENE + 0.25*BPINENE + 0.1*DLIMONENE + 0.15*3-CARENE + 0.1*SABINENE. Following MCM, we use APINENE = 0.2*SCI3, BPINENE =0.148*SCI1 + 0.102*SCI3, DLIMONENE = 0.135*SCI3. SCI yields for 3-CARENE and SABINENE are not available in MCM. Ma et al. (2009) suggested that SCI yield for 3-CARENE should be lower than APINENE. For this work, we assume that it is equal to that of APINENE. For SABINENE, we assume that SCI yield is equal to that of BPINENE since their structures are similar.

Figures

Figure 1: (a) Predicted monthly mean SO_4^{2-} concentrations without SCI in January (b) SCI initiated monthly mean enhancements in January (c) predicted monthly mean SO_4^{2-} concentrations without SCI in July (d) SCI initiated monthly mean enhancements in July. Biogenic emissions derived from BEIS. Observed values occurring within the area outlined in Figure 1(b) are averaged for Figure 2. Observed values occurring within the area outlined in Figure 1(b) are also used for comparing predicted SO_4^{2-} with observed data in Figures 5(a-c) and 6(a-c).

Figure 2: (a) Time series of predicted daily mean enhanced SO_4^{2-} due to the SCI chemistry and SO_2 x SCI3/20 for the area shown in Figure 1(d) (b) diurnal changes of predicted SO_4^{2-} without and with the SCI chemistry along with HO and SCI3 for the same area. BEIS emissions were used. SO_2 x SCI3 has been divided by 20 and SO_4^{2-} by 60 to fit into scale.

Figure 3: (a) Predicted monthly mean SO_4^{2-} concentrations in July without SCI chemistry (MEGAN emissions) (b) SCI initiated monthly mean SO_4^{2-} enhancements in July (MEGAN emissions). Area outlined in black rectangle in Figure 3(b) is the area over which predicted SO_4^{2-} concentrations are compared with observed data in Figures 5(d-f) and 6(d).

Figure 4: (a) Predicted daily mean SO_4^{2-} concentration on July 1 without SCI chemistry (b) SCI initiated daily mean enhancements with Mauldin et al. (2012) reported rate constant (c) SCI initiated daily mean enhancement with Welz et al. (2012) reported rate constant (d) SCI initiated daily mean enhancements obtained with the Mauldin et al. (2012) reported value as "net" rate constant [the rate constant reported by Mauldin et al. (2012) for the SO_2+SCI3 reaction was used as "net" rate constant without any loss of SCI3 by reactions with H_2O, $(H_2O)_2$, and NO_2] (e) SCI initiated daily mean enhancement with Welz et al. (2012) reported rate constant for SO_2+SCI reactions and the lowest rate constant for the SCI3+H_2O reaction (f) SCI initiated daily mean enhancement with Welz et al. (2012) reported rate constant for SO_2+SCI reactions, the lowest rate constant for the SCI3+H_2O reaction, and unimolecular decomposition of SCIs. Biogenic emissions are derived from BEIS.

Figure 5: A comparison of predicted SO_4^{2-} concentrations to observations from the CASTNET sites (top) the IMPROVE sites (second from top) the CSN sites (2^{nd} from bottom) the SEARCH sites (bottom). Results from model runs using BEIS emission are shown in left-hand panels and results from model runs using MEGAN emissions are shown in right-hand panels. Observed values occurring within the areas outlined in Figures 1(d) and 3(b) are used for comparing predicted SO_4^{2-} with observed data in left and right-hand plots, respectively. Circle, square, and triangle symbols depict the median value across all sites for each date, while whiskers extend to the 25^{th} and 75^{th} percentile values at locations of monitoring sites for each date.

Figure 6: A comparison of predicted mass fraction of sulfur in SO_4^{2-} (BEIS emissions) to observed data from CASTNET sites in January (top left), July (bottom left), and August (top right), and a comparison of predicted mass fraction of sulfur in SO_4^{2-} (MEGAN emissions) to observed data from CASTNET sites in July (bottom right). Observed values occurring within the areas outlined in Figures 1(d) and 3(b) are used for comparing predicted SO_4^{2-} with observed data in BEIS emissions and MEGAN emissions panels, respectively. Centerline of the boxplots shows the mean modeled value for each bin of observed values. Boxes extend to 25^{th} and 75^{th} percentile values, whiskers extend to 1.5 times the interquartile range, and dots show outlier values.

Figure 7: A comparison of predicted mass fraction of sulfur in SO_4^{2-} (BEIS emissions) to observed data from SEARCH sites in January (top left), July (bottom left), and August (top right), and a comparison of predicted mass fraction of sulfur in SO_4^{2-} (MEGAN emissions) to observed data from SEARCH sites in July (bottom right). Observed values occurring within the areas outlined in Figures 1(d) and 3(b) are used for comparing predicted SO_4^{2-} with observed data in BEIS emissions and MEGAN emissions panels, respectively. Centerline of the boxplots shows the mean modeled value for each bin of observed values. Boxes extend to 25^{th} and 75^{th} percentile values, whiskers extend to 1.5 times the interquartile range, and dots show outlier values.

720 **Figure 1:** (a) Predicted monthly mean SO_4^{2-} concentrations without SCI in January (b) SCI initiated monthly mean
721 enhancements in January (c) predicted monthly mean SO_4^{2-} concentrations without SCI in July (d) SCI initiated
722 monthly mean enhancements in July. Biogenic emissions derived from BEIS. Observed values occurring within the
723 area outlined in Figure 1(b) are averaged for Figure 2. Observed values occurring within the area outlined in Figure
724 1(b) are also used for comparing predicted SO_4^{2-} with observed data in Figures 5(a-c) and 6(a-c).
725

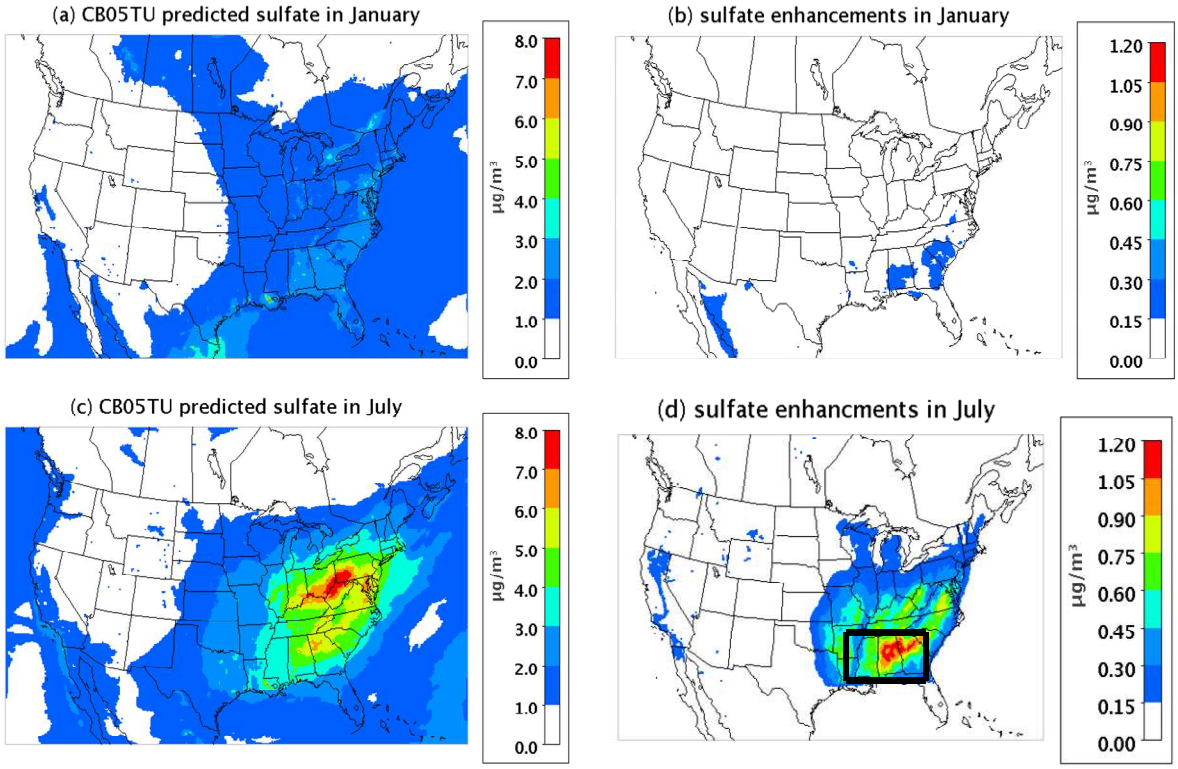

726

Figure 2: (a) Time series of predicted daily mean enhanced SO_4^{2-} due to the SCI chemistry and SO_2 x SCI3/20 for the area shown in Figure 1(d) (b) diurnal changes of predicted SO_4^{2-} without and with the SCI chemistry along with HO and SCI3 for the same area. BEIS emissions were used. SO_2 x SCI3 has been divided by 20 and SO_4^{2-} by 60 to fit into scale.

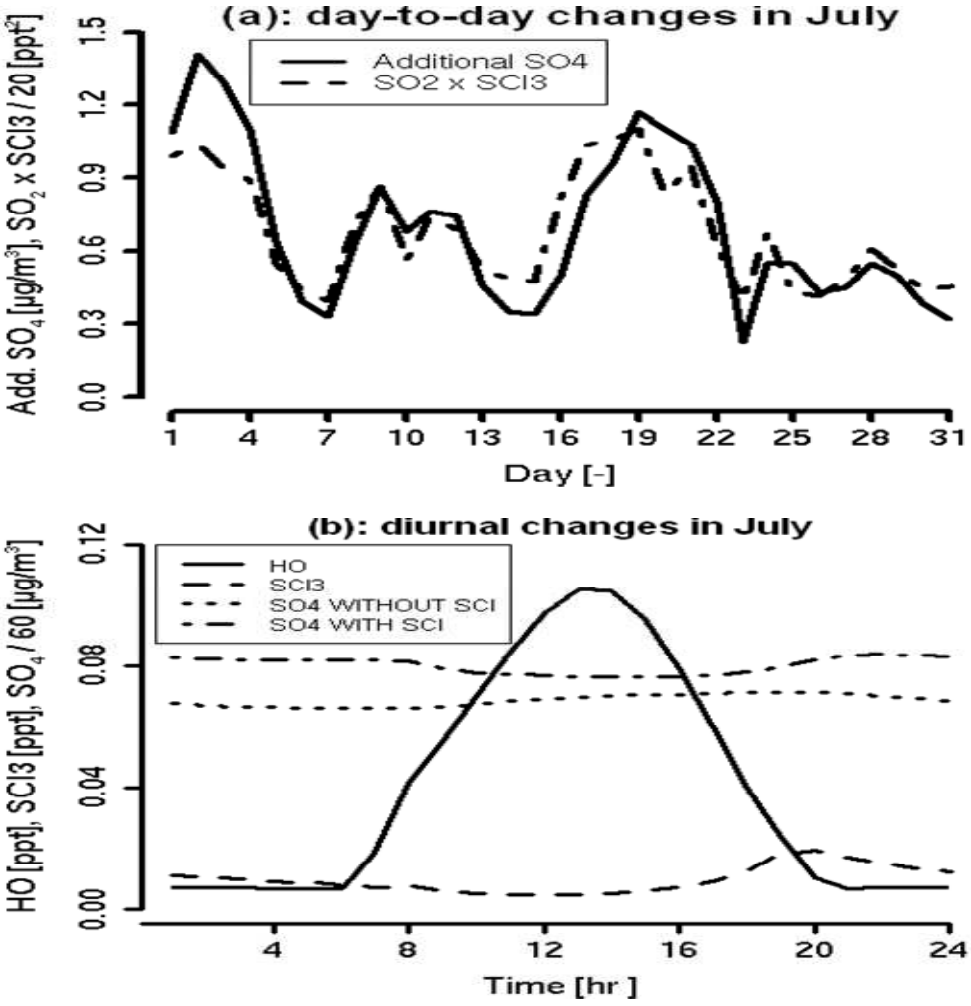

Figure 3: (a) Predicted monthly mean SO_4^{2-} concentrations in July without SCI chemistry (MEGAN emissions) (b) SCI initiated monthly mean SO_4^{2-} enhancements in July (MEGAN emissions). Observed values occurring within the area outlined in Figure 3(b) are used for comparing predicted SO_4^{2-} with observed data in Figures 5(d-f) and 6(d).

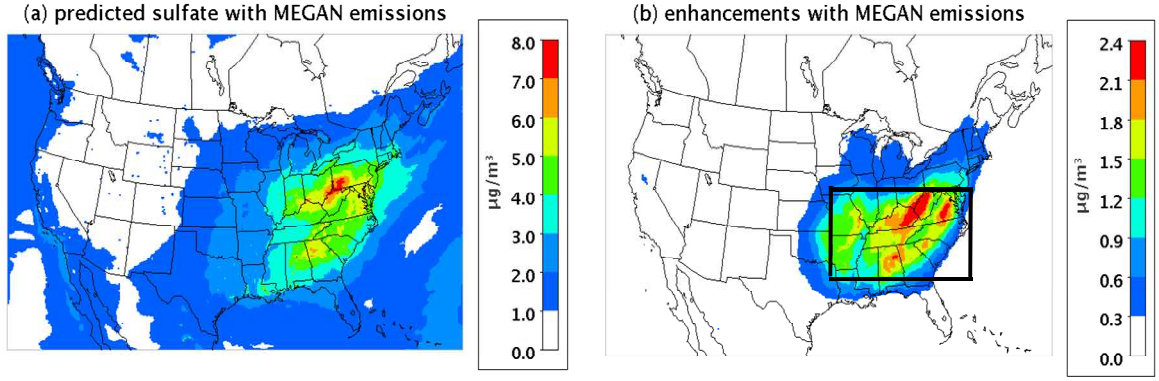

Figure 4: (a) Predicted daily mean SO_4^{2-} concentration on July 1 without SCI chemistry (b) SCI initiated daily mean enhancements with Mauldin et al. (2012) reported rate constant (c) SCI initiated daily mean enhancement with Welz et al. (2012) reported rate constant (d) SCI initiated daily mean enhancements obtained with the Mauldin et al. (2012) reported value as "net" rate constant [the rate constant reported by Mauldin et al. (2012) for the SO_2+SCI3 reaction was used as "net" rate constant without any loss of SCI3 by reactions with H_2O, $(H_2O)_2$, and NO_2] (e) SCI initiated daily mean enhancement with Welz et al. (2012) reported rate constant for SO_2+SCI reactions and the lowest rate constant for the SCI3+H_2O reaction (f) SCI initiated daily mean enhancement with Welz et al. (2012) reported rate constant for SO_2+SCI reactions, the lowest rate constant for the SCI3+H_2O reaction, and unimolecular decomposition of SCIs. Biogenic emissions are derived from BEIS.

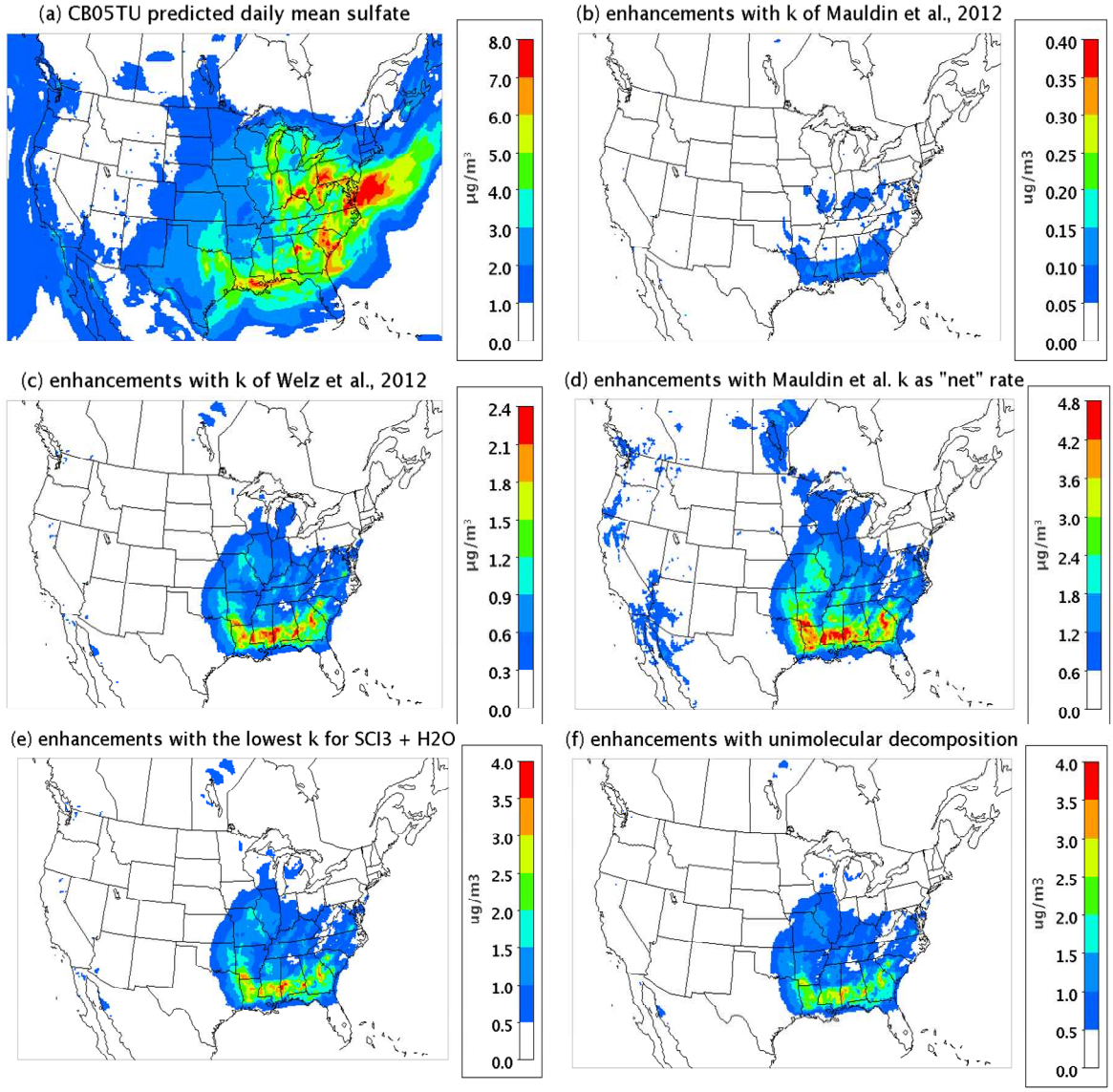

Figure 5: A comparison of predicted SO_4^{2-} concentrations to observations from the CASTNET sites (top) the IMPROVE sites (second from top) the CSN sites (2nd from bottom) the SEARCH sites (bottom). Results from model runs using BEIS emission are shown in left-hand panels and results from model runs using MEGAN emissions are shown in right-hand panels. Observed values occurring within the areas outlined in Figures 1(d) and 3(b) are used for comparing predicted SO_4^{2-} with observed data in left and right-hand plots, respectively. Circle, square, and triangle symbols depict the median value across all sites for each date, while whiskers extend to the 25th and 75th percentile values at locations of monitoring sites for each date.

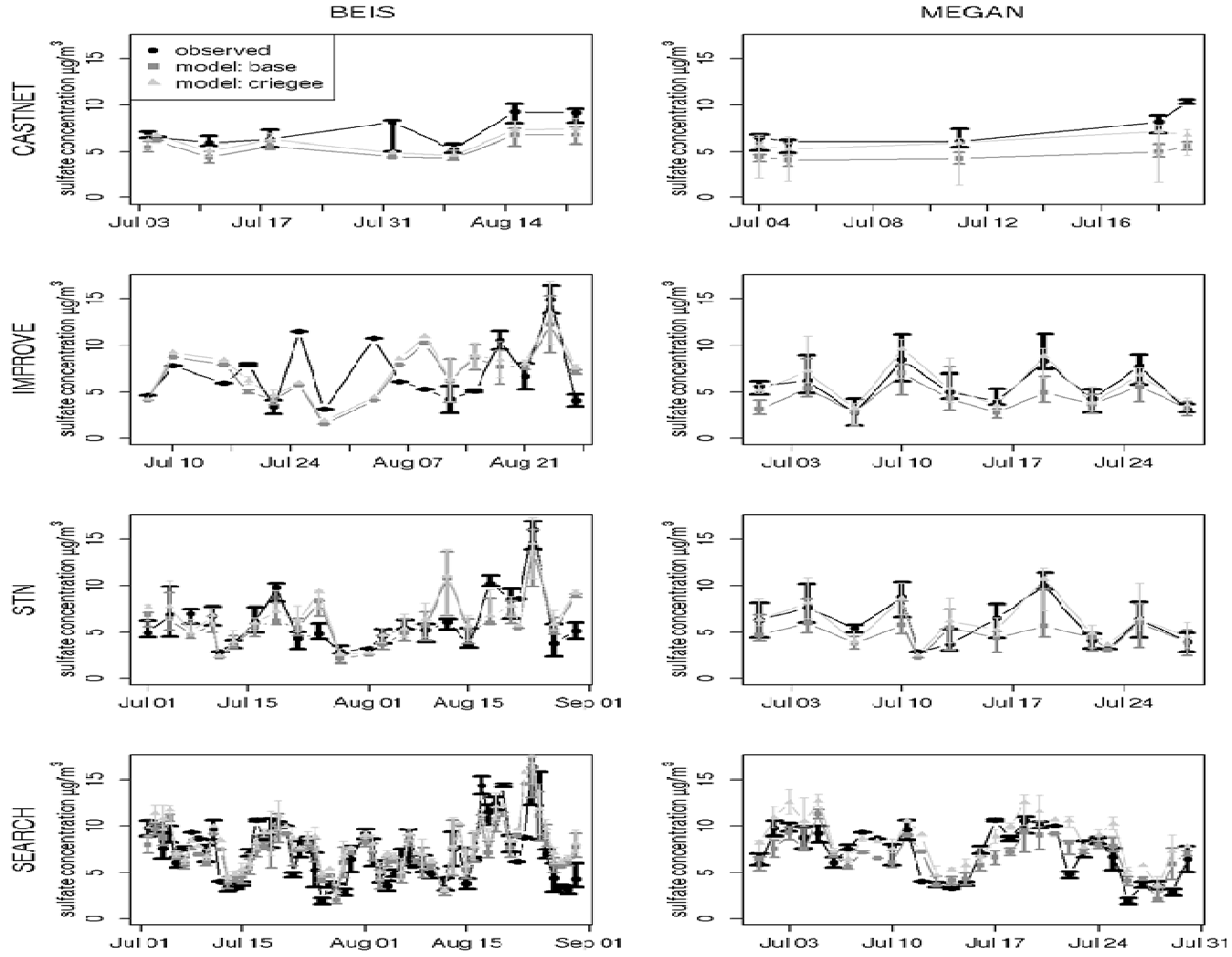

Figure 6: A comparison of predicted mass fraction of sulfur in SO_4^{2-} (BEIS emissions) to observed data from CASTNET sites in January (top left), July (bottom left), and August (top right), and a comparison of predicted mass fraction of sulfur in SO_4^{2-} (MEGAN emissions) to observed data from CASTNET sites in July (bottom right). Observed values occurring within the areas outlined in Figures 1(d) and 3(b) are used for comparing predicted SO_4^{2-} with observed data in BEIS emissions and MEGAN emissions panels, respectively. Centerline of the boxplots shows the mean modeled value for each bin of observed values. Boxes extend to 25th and 75th percentile values, whiskers extend to 1.5 times the interquartile range, and dots show outlier values.

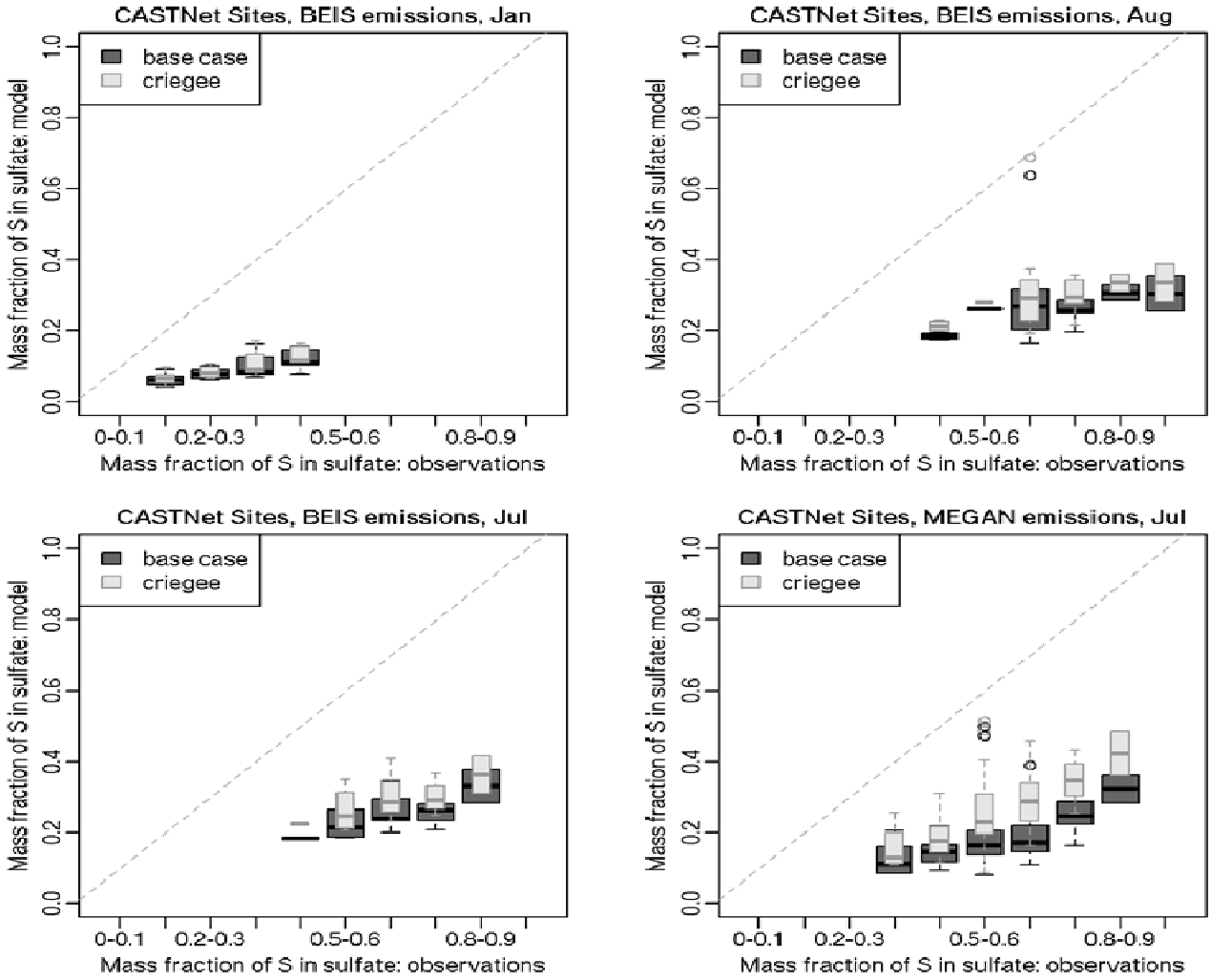
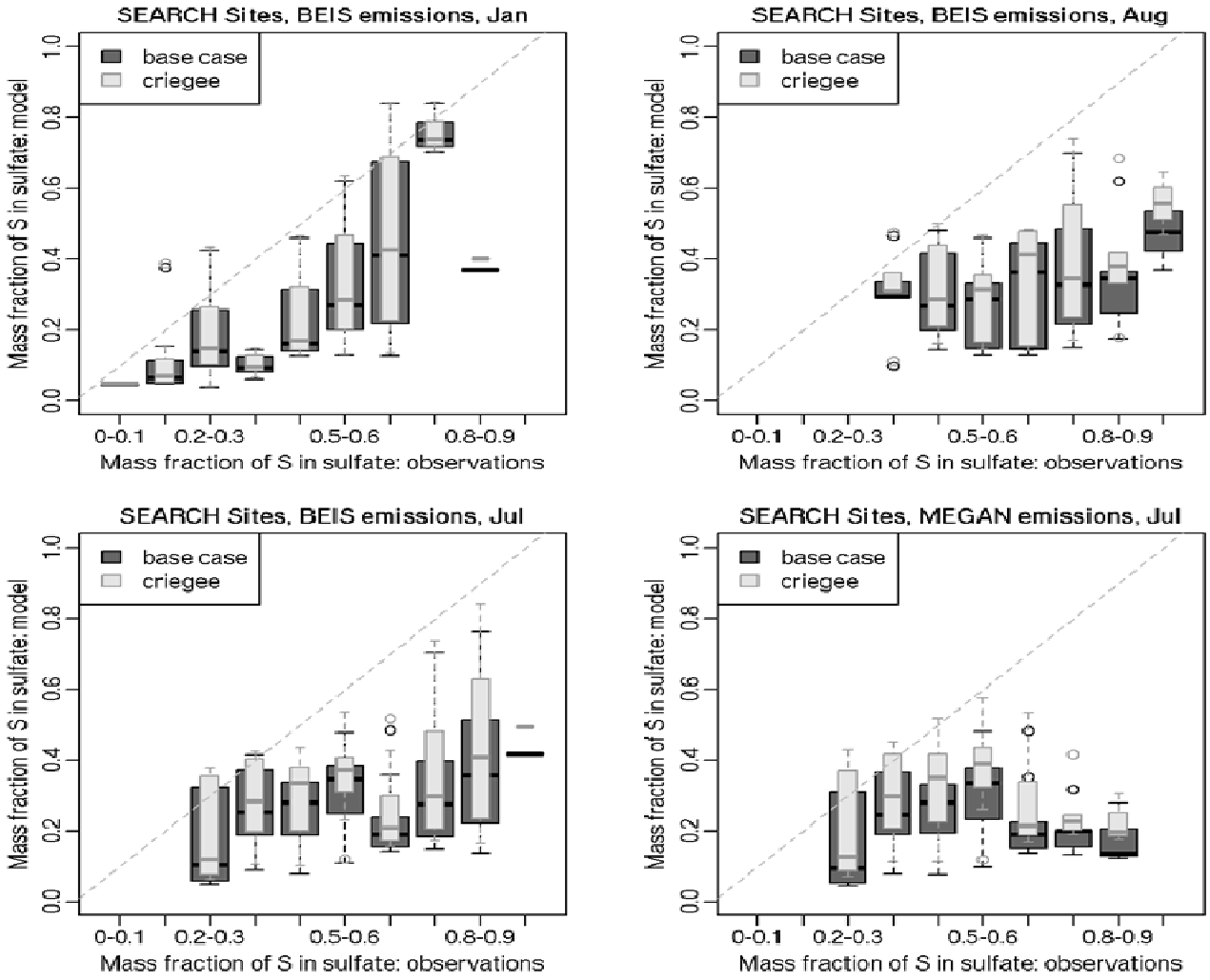
Figure 7: A comparison of predicted mass fraction of sulfur in SO_4^{2-} (BEIS emissions) to observed data from SEARCH sites in January (top left), July (bottom left), and August (top right), and a comparison of predicted mass fraction of sulfur in SO_4^{2-} (MEGAN emissions) to observed data from SEARCH sites in July (bottom right). Observed values occurring within the areas outlined in Figures 1(d) and 3(b) are used for comparing predicted SO_4^{2-} with observed data in BEIS emissions and MEGAN emissions panels, respectively. Centerline of the boxplots shows the mean modeled value for each bin of observed values. Boxes extend to 25th and 75th percentile values, whiskers extend to 1.5 times the interquartile range, and dots show outlier values.